RSC Advances

PAPER

View Article Online
View Journal | View Issue

Cite this: *RSC Adv.*, 2024, **14**, 16278

Construction of a pillar[5]arene-based supramolecular chiral polymer linked to aminophosphine salt for chiral recognition of enantiomers of mandelic acid†

Chong Lin,[a] Yang Shen,[a] Xiaojun Guo,[a] Wengui Duan,[a] Yan Huang,*[b] Guobao Huang*[c] and Luzhi Liu *[ac]

In recent years, supramolecular chirality has been greatly developed in asymmetric synthesis, chiral sensing and other research fields, but its application in molecular chiral recognition has not been extensively studied. In this paper, *L*-Boc-tyrosine methoxyester and phosphorus chloride salts were introduced into the framework of pillar[n]arene, and a pillar[5]arene-based supramolecular chiral polymer ***L*-TPP-P** was constructed. The supramolecular polymer had stable supramolecular chiral properties and could be used as a chiral solvation reagent for chiral recognition of mandelic acid **MA**. The molar ratio method and Scatchard plot showed that the complexation ratio of ***L*-TPP-P** (pillar[5]arene monomer as the reference object) and **MA** was 1 : 1, and the complexation constants of ***L*-TPP-P** with ***R*-MA** and ***S*-MA** were 4.51 × 10^5 M^{-1} and 6.5 × 10^4 M^{-1}, respectively. The significant affinity difference of ***L*-TPP-P** for different enantiomers of **MA** showed the excellent chiral recognition and stereoselectivity of pillar[5]arene-based supramolecular polymers for **MA**. This study provides a new idea for a novel supramolecular polymer chiral recognition reagent or chiral recognition method.

Received 23rd February 2024
Accepted 9th May 2024

DOI: 10.1039/d4ra01386g

rsc.li/rsc-advances

1. Introduction

Supramolecular chirality is mainly generated by multiple non-covalent interactions as a result of molecular self-assembly,[1,2] playing a crucial role in natural biological systems and advanced materials.[3] Potential applications of various supramolecular chiral systems include chiral sensing,[4] asymmetric synthesis,[5] chiral gelling gels,[6] chiral optical switches,[7] chiral recognition,[8] and so on. Chiral molecules exhibit significant differences in activity and toxicity in many life activities. Therefore, realizing chiral recognition of enantiomers is of great significance in the field of analytical assays.[9] Currently, many studies have shown that, the host molecule selectively binds to the enantiomer of the guest molecule through non-covalent interactions such as hydrogen bonding,[10] metal coordination, π–π packing,[11] and/or electrostatic interactions.[12] So a number of chiral systems are reported for enantioselective recognition and separation, such as chiral metal–ligand complexes,[13] chiral polymers,[14] micelles,[15] and vesicles.[16] Supramolecular chiral polymers, as a good host material, provide more possibilities for chiral recognition.[17]

In recent years, novel macrocyclic host molecules have been synthesized continuously, and their unique molecular recognition characteristics have promoted the development of supramolecular chemistry.[18] The key to molecular recognition of chiral supramolecules is the perfect cooperation between the guest molecule and the host supramolecule, so it is particularly important to select suitable chiral supramolecules as host materials for efficient chiral recognition.[19] Pillar[*n*]arenes, as a new type of supramolecular macrocyclic compounds, have attracted attention from scientific researchers in just over a decade due to their hydrophobic electron-rich cavity structure, inherent planar chiral configuration, easy functionalization and excellent host–guest properties.[20] It is possible to inhibit the rotation of pillar[*n*]arene by introducing bulky substituents on both rings to obtain planar chiral *pR*- and *pS*- forms of pillar[*n*]arene enantiomers.[21] In addition, pillar[*n*]arenes can induce chiral signals and amplify chiral molecules through host–guest interactions, so that chiral molecules can be detected,[22] so pillar[*n*]arenes have great application potential in chiral recognition.[23]

[a]*Guangxi Colleges and Universities Key Laboratory of Applied Chemistry Technology and Resource Development, School of Chemistry and Chemical Engineering, Guangxi University, Nanning 530004, China. E-mail: llzh068@163.com*

[b]*Guangxi Institute of Chinese Traditional Medical & Pharmaceutical Science, Guangxi Key Laboratory of Traditional Chinese Medicine Quality Standards, Nanning, China. E-mail: hy2002-2006@163.com*

[c]*Guangxi Key Lab of Agricultural Resources Chemistry and Biotechnology, College of Chemistry and Food Science, Yulin Normal University, Yulin, Guangxi 537000, PR China. E-mail: lzjx0915@163.com*

† Electronic supplementary information (ESI) available. See DOI: https://doi.org/10.1039/d4ra01386g

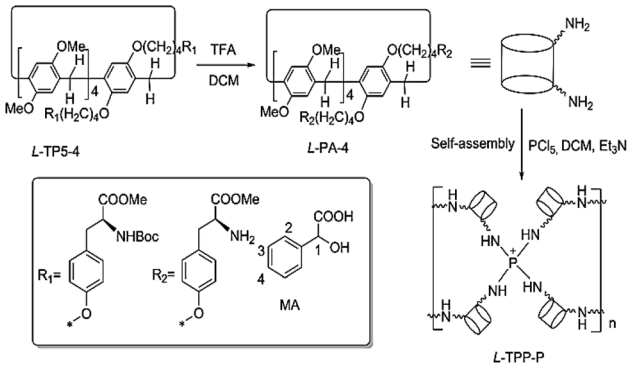

Scheme 1 The synthetic route of *L*-TPP-P.

In our previous study,[24] we found that the introduction of a large chiral group could promote the generation of a microchiral environment. The strong shielding effect of the cavity could result in differentiation of the proton signals of the guest in the diastereomeric complexes with the pillar[5]arene, enabling the detection of multiple proton signals in the substrate. One of the greatest advantages of the deshielding strategy over the shielding strategy was that the size of the identified guest was not limited by the volume of the cavity. Our previously developed tyrosine-modified pillar[5]arene molecule successfully recognized and identified the enantiomers of aromatic amines by the shielding effect of the cavity.[24] More importantly, the NHBoc group of the tyrosine-based pillar[5]arene was located outside its cavity, which can be exploit to create an NMR reagent for chiral identification using the deshielding strategy. In addition, chiral aminophosphonium salts showed high enantioselective recognition of various chiral guest molecules with functional groups, such as carboxylic acids, amines, and alcohols.[25] Therefore, we constructed a supramolecular polymer ***L*-TPP-P** by combining a tyrosine-modified chiral pillar[5]arene with an aminophosphine salt, hoping that the host–guest binding site could be controlled in the deshielded region to achieve guest chiral recognition by combining the NH_2 group outside the cavity with phosphine ions (Scheme 1). Here, mandelic acid (**MA**) was used as a model for chiral drug enantiomeric selective recognition. In order to achieve chiral recognition of **MA** enantiomers, chiral induction and amplification of ***L*-TPP-P** were studied. Compared with pillar[5]arene monomer ***L*-PA-4**, ***L*-TPP-P** exhibited excellent recognition ability for mandelic acid enantiomers.

2. Experimental

The infrared spectra (KBr particle method) were recorded on the Nicolet is 50 FT-IR spectrometer (Thermo Scientific Co., Ltd, Madison, WI, USA). ^{1}H NMR, ^{13}C NMR spectra were recorded in $CDCl_3$ solvent on Bruker Avance III HD 600 MHz spectrometer (Bruker Ltd, Zurich, Switzerland). The chemical shifts were expressed in ppm (δ) relative to TMS as internal standard. Other reagents were purchased from commercial suppliers and used as received. The mass spectra were recorded on a TSQ Quantum Access MAX HPLC-MS instrument (Thermo Scientific Co., Ltd, Waltham, MA, USA). Melting points were determined on a MP420 automatic melting point apparatus (Hanon Instruments Co., Ltd, Jinan, China), and were not corrected. SEM was recorded on scanning electron microscope (TESCAN MIRA LMS, Czech). Other reagents were purchased from commercial suppliers and used as received.

2.1 Synthesis of compound *L*-PA-4

***L*-TP5-4** (100 mg, 0.071 mmol) was dissolved in 8 mL dichloromethane, trifluoroacetic acid (3 mL) was added, and the reaction time was 1 h at 25 °C, and TLC was used to follow the reaction. The reacted solution was placed in a dialysis bag with a MWCO of 1000 and water was changed at half hour, four hours and six hours and the reaction was followed by TLC. After drying, ***L*- PA-4** was obtained as a white solid in 76% yield. ***L*-PA-4** melting point: 134.4–141.6 °C; $[\alpha]_{L\text{-PA-4}} = 36.8400$; IR (KBr) cm^{-1}: 3424.05 (N–H), 2937.58, 2851.77 (C–H), 1501.34 (Ar–C=C), 1212.06, 1046.69 (Ar–O, C–O); ^{1}H NMR (600 MHz, chloroform-*d*) δ 9.55 (s, 4H, H-n), 7.09 (d, 4H, H-i), 6.87–6.81 (d, 4H, H-h), 6.79–6.74 (m, 10H, H-a), 4.00 (t, J = 5.9 Hz, 4H, H-d), 3.92–3.87 (t, 6H, H-g, k), 3.77 (s, J = 7.1, 5.9 Hz, 6H, H-m), 3.73 (s, 10H, H-b), 3.64 (s, J = 17.9, 6.0 Hz, 24H, H-c), 3.04 (dd, J = 13.7, 5.2 Hz, 2H, H-j), 2.83 (dd, J = 13.7, 7.7 Hz, 2H, H-j), 1.85 (m, 8H, H-e, f); ^{13}C NMR (151 MHz, chloroform-*d*) δ168.50, 151.44, 150.27, 140.88, 140.82, 130.24, 128.98, 127.59, 121.07, 119.18, 114.55, 113.62, 67.43, 56.15, 55.57, 51.95, 47.48, 44.24, 43.94, 42.48, 40.68, 40.16, 29.85, 29.81, 29.74, 29.71, 29.67, 29.63, 26.29, 26.08; HRMS (ESI) *m*/*z*: calcd for $[C_{71}H_{84}N_2O_{16} + H]^+$, 1221.5894; found: 1221.58923.

2.2 Synthesis of compound *L*-TPP-P

***L*-PA-4** (15 mg, 0.0124 mmol, 2 equiv.) and triethylamine (0.5 mL) were added to dichloromethane (3 mL) and stirred for 12 hours at 25 °C. Then phosphorus pentachloride (1.2 mg, 0.0062 mmol, 1 equiv.) was dissolved in 2 mL dichloromethane and added to the mixed solution and reacted at room temperature for 24 h. The solution obtained from the reaction was evaporated to dryness and purified by washing with deionized water (0.5 mL) and ether (0.5 mL) to obtain ***L*-TPP-P** as a white solid in 86% yield. IR (KBr) cm^{-1}: 3475.69, 3398.14 (N–H), 3039.19 (Ar–H), 2934.87, 2851.75 (C–H), 1740.99 (C=O), 1502.21, 1468.27 (Ar–C=C), 1214.45, 1045.79 (Ar–O, C–O); ^{1}H NMR (600 MHz, chloroform-*d*) δ 9.51 (s, 2H, H-n), 7.11–7.05 (d, 4H, H-i), 6.87–6.80 (d, 4H, H–h), 6.80–6.71 (m, 10H, H-a), 4.00 (t, J = 5.9 Hz, 4H, H-d), 3.88 (t, 6H, H-g, k), 3.78–3.74 (s, 6H, H-m), 3.74–3.68 (s, 10H, H-b), 3.67–3.59 (s, 24H, H-c), 3.03 (dd, J = 13.7, 5.2 Hz, 2H, H-j), 2.82 (dd, J = 13.7, 7.8 Hz, 2H, H-j), 1.87 (m, 8H, H-e, f). ^{13}C NMR (151 MHz, Chloroform-*d*) δ 123.91, 123.41, 123.41, 115.88, 56.07, 56.06, 52.86, 52.62, 45.52, 34.67, 34.67, 34.19, 34.19, 31.86, 31.86, 31.56, 29.63, 29.59, 29.30, 29.30, 22.63, 22.63, 14.05, 7.96, 7.55. ^{31}P NMR (600 MHz, chloroform-d) δ −17.57 (s, 1P).

3. Results and discussion

3.1 Preparation and characterization of pillar[5]arenes-based supramolecular chiral polymer *L*-TPP-P

Their syntheses were shown in Scheme 1. The intermediates and target compounds were characterized by ^{1}H NMR

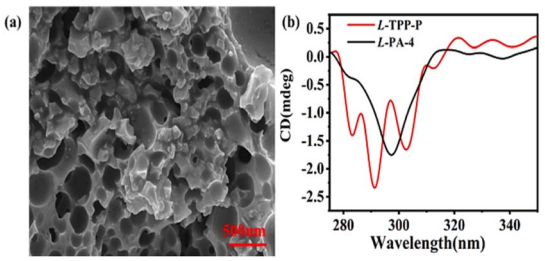

Fig. 1 (a) SEM spectra of *L*-TPP-P; (b) CD spectra of *L*-PA-4 and *L*-TPP-P in $CHCl_3$.

spectroscopy, ^{13}C NMR spectroscopy, ^{31}P NMR spectroscopy, IR spectroscopy and HRESI-MS (Fig. S2–S9†). As shown in Fig S3 and S7,† compared with ***L*-PA-4**, the proton peak of benzene ring (δ = 6.80–6.71) and methyl group (δ = 3.78–3.74) in ***L*-TPP-P** were significantly wider and cleaved into multiple small peaks indicating that the polymer ***L*-TPP-P** had been synthesized.[26] In ^{31}P NMR (Fig. S9†), the chemical shift was −17.57 ppm and only one single peak appeared, indicating that the reaction was relatively thorough, the supramolecular chiral polymer ***L*-TPP-P** was successfully synthesized. Its porous structure was observed by SEM (Fig. 1a). We tested the CD signals of ***L*-TPP-P** and ***L*-PA-4** by circular dichroic spectroscopy in $CHCl_3$ (Fig. 1b). Compared with monomer ***L*-PA-4**, ***L*-TPP-P** had a CD signal and was stronger and wider, indicating that ***L*-TPP-P** had chirality and may have chiral recognition ability.

3.2 Study the chiral recognition effect of *L*-TPP-P with MA by ^{1}H NMR

Since supramolecular polymers ***L*-TPP-P** and **MA** had good solubility, strong non-covalent bond interaction and low solvent proton signal interference in $CDCl_3$, ***L*-TPP-P** was first selected as the CSA of classical model molecule **MA** in $CDCl_3$ to explore its chiral recognition.

The splitting degree was expressed by the change of nonequivalent chemial shifts ($\Delta\Delta\delta$). The chiral recognition was carried out at a molar ratio of ***L*-TPP-P** to (±)**MA** of 1 : 1, as shown in Fig. S10b.† In the presence of ***L*-TPP-P**, the peak and chemical shift of (±)**MA** changed significantly. The chemical shift of H^2 shifted to the low field ($\Delta\delta H^2$ = 0.169 ppm) and showed baseline separation ($\Delta\Delta\delta H^2$ = 0.021 ppm, ● represents the *R*-configuration, ○ represents the *S*-configuration) with an integration ratio of 1 : 1. At the same time, the P chemical shift shifted towards a higher field ($\Delta\delta$ = 0.4227 ppm, Fig. S11†). Further chiral identification of ***L*-TPP-P** by varying the different enantiomeric excesses of **MA** showed that the chemical shifts of H^2 in the *R* configuration were in a lower field relative to the *S* configuration (Fig. 2). Furthermore, the chemical shift or signal change of the proton H^2 was dependent on the **MA** enantiomer ratio, which could be attributed to the fact that the different enantiomeric excesses of the guests influenced their host–guest interaction behaviors with the polymers of the components of ***L*-TPP-P**. The host ***L*-TPP-P** was more complex than a single compound, consisting of several polymers with varying molecular weights that could have varied shielding or deshielding

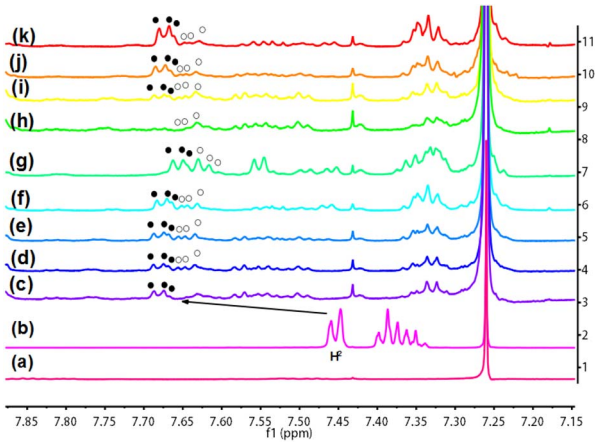

Fig. 2 Partial NMR spectra of **MA** with various enantiomeric excess (a) *L*-TPP-P, (b) ±**MA**, (c) R/S = 5 : 0, (d) R/S = 5 : 1, (e) R/S = 5 : 2, (f) R/S = 5 : 3, (g) R/S = 5 : 5, (h) R/S = 0 : 5, (i) R/S = 1 : 5, (j) R/S = 2 : 5, (k) R/S = 3 : 5 in the presence of *L*-TPP-P in $CDCl_3$. (● represents the *R* configuration, ○ represents the *S* configuration).

effects on the guest. This could cause protons' chemical shifts to move to higher or lower fields, even weaken their NMR signals, causing them to broaden or even disappear into the baseline.[27]

These results indicated that ***L*-TPP-P** showed good enantiomer recognition for **MA**. The electrostatic interaction between the phosphine cation of ***L*-TPP-P** and the carboxyl anion of **MA** was the main driving force for host–guest interaction, and it also effectively prevented **MA** from entering the shielded region of the cavity, meaning that the supramolecular polymer may also be suitable for recognizing larger guest without being affected by the cavity size of pillar[*n*]arene. It should note that **MA** could interact with the monomer ***L*-PA-4** through H-bonding, so the **MA** proton signal shifted to downfield. But unfortunately ***L*-PA-4** had no chiral recognition for **MA** (Fig. S10a†). Thus ***L*-TPP-P** was identified as an effective chiral recognition reagent and subsequent studies were carried out.

3.3 Study the main driving force for host–guest interaction by FT-IR

In order to investigate the main driving force for host–guest interaction, the systems were also analyzed by IR spectroscopy. After the host–guest interaction between the ***L*-TPP-P** and **MA**, the IR measurements (Fig. S13†) revealed that the frequency of the asymmetric stretching vibration of C=O group of MA increased significantly from 1727 cm^{-1} to 1747 cm^{-1}, whereas the characteristic frequency of O–H decreased significantly from 3448 cm^{-1} to 3420 cm^{-1}. These results clearly demonstrated that the carboxylate negative ions of the mandelic acid and the *ortho*-phosphorus ions of the supramolecular polymer had strong electrostatic interactions, which is consistent with the previous NMR analysis. Moreover, the residues of tyrosine in the system could also form hydrogen bonds with OH or COOH of **MA**. That is, the chiral recognition of pillararene-based supramolecular polymers was achieved through the synergistic combination of stereoselectivity and differential

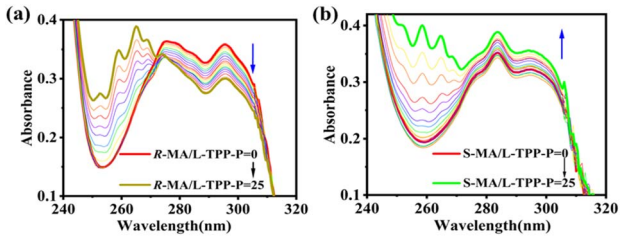

Fig. 3 UV spectra of *L*-TPP-P with (a) *R*-MA and (b) *S*-MA in solution [*L*-TPP-P] = 0.01 mM.

signal amplification. Amino acid residues played a key role in chiral recognition.

3.4 Study the complexing properties of *L*-TPP-P with MA by UV

To study the complexation properties between the host and guest, the UV absorption spectra of the host ***L*-TPP-P** mixed with the guest **MA** of different configurations were scanned by UV spectrophotometer. As shown in Fig. 3a and b, when ***L*-TPP-P** was mixed with ***R*-MA** or ***S*-MA**, the UV absorption intensities of the system at 257–270 nm increased dramatically and accompanied by the generation of three new absorption peaks. It indicated that ***L*-TPP-P** had an excellent host–guest interaction with ***R*-MA** and ***S*-MA**. For the ***R*-MA** @ ***L*-TPP-P** system, its absorbance at 273–310 nm gradually decreased as the guest concentration increased. On the contrary, the UV absorption of

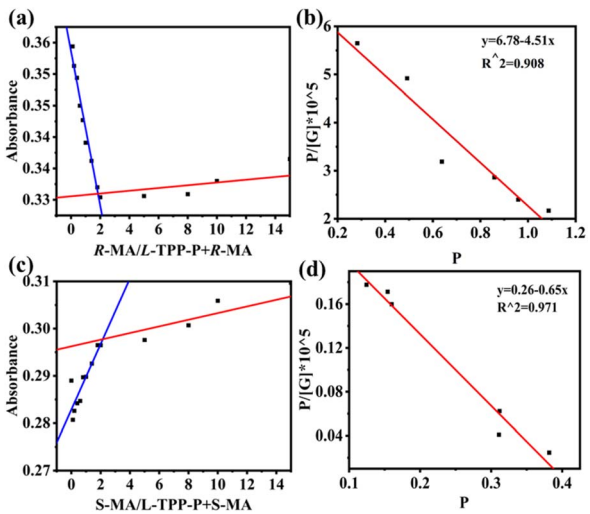

Fig. 4 Mole ratio plot for *L*-TPP-P (pillar[5]arene monomer as a reference) and MA, indicating 1 : 1 stoichiometry (a) *R*-MA, (c) *S*-MA; the non-linear curve-fitting (UV titrations) for the host–guest complexation of *L*-TPP-P (0.01 mM) with different concentration of MA, (b) the association constant (K_R) was calculated to be about 4.51×10^5 M^{-1}; (d) the association constant (K_S) was calculated to be about 6.5×10^4 M^{-1}. P ($P = \Delta A/\Delta A_0$) was used as the horizontal coordinate, ΔA was the value of change in absorbance after any ratio of complexation, ΔA_0 was the value of change in absorbance for complete complexation, and the vertical coordinate was P/[MA].

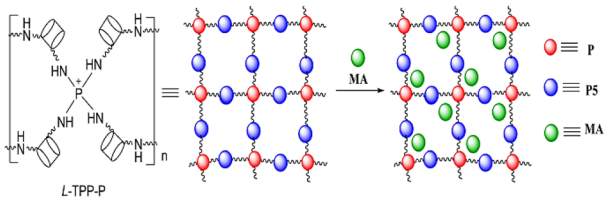

Fig. 5 Complex mode of *L*-TPP-P and MA. P5: pillar[5]arene unit.

the ***S*-MA** @ ***L*-TPP-P** system increased as guest concentration increased. It demonstrated that the complexation characteristics of ***L*-TPP-P** varied depending on the MA configuration and thus could be utilized for chiral identification by UV absorption spectra. In addition, the stoichiometry of complexation between ***L*-TPP-P** and ***R*-MA** and ***S*-MA** were investigated by the Job plot method (*i.e.*, UV titration experiments), and it was found that the binding stoichiometry of the host–guest complexes, ***R*-MA** @ ***L*-TPP-P** and ***S*-MA** @ ***L*-TPP-P**, were both 1 : 1 (Fig. 4a and c). After determining the binding ratios, their binding constants (K_a) were calculated to be 4.51×10^5 M^{-1} (K_R) and 6.5×10^4 M^{-1} (K_S), respectively. This indicated that ***L*-TPP-P** had a higher affinity for ***R*-MA** compared to ***S*-MA** ($K_R/K_S = 6.9$).

3.5 The complexation mode of *L*-TPP-P and MA

Since the complexation ratio of the host ***L*-TPP-P** (pillar[5]arene monomer as a reference) and the guest **MA** was 1 : 1, *i.e.*, the binding ratio of **MA**/P^+ was 2 : 1. It was speculated that the carboxyl anion group of two guest **MA** were attracted to a phosphine cation group on the host ***L*-TPP-P** by electrostatic interaction, thus forming a supramolecular system, and the complexation model was shown in Fig. 5.

4. Conclusions

In conclusion, we have developed a new tyrosine-modified pillar[5]arenes supramolecular chiral polymer ***L*-TPP-P**. This supramolecular polymer possessed stable supramolecular chirality and could be employed as a chiral solvating agent for the enantiomer recognition of **MA**. In the presence of ***L*-TPP-P**, the proton peak and chemical shift of H^2 in **MA** changed significantly, and the baseline separation of proton signals of different configurations was realized. The complexation ratios of ***L*-TPP-P** (pillar[5]arene monomer as a reference) with both ***R*-MA** and ***S*-MA** were 1 : 1, and their complexation constants were 4. 51×10^5 M^{-1} and 6.5×10^4 M^{-1}, with their $K_R/K_S = 6.9$, indicating that ***L*-TPP-P** had good stereoselectivity for **MA** with different configurations. Importantly, polymer monomer ***L*-PA-4** had not demonstrated chiral recognition of **MA**, and supramolecular chiral polymers had great potential for application in chiral recognition, complementing well the chiral recognition of traditional small molecules. This study is expected to provide a strategy for highly enantioselective recognition of chiral drugs, as well as new ideas for novel supramolecular polymer chiral recognition reagents or chiral recognition methods.

Conflicts of interest

The authors declare no conflict of interest.

Acknowledgements

We gratefully thank the financial support of the National Natural Science Foundation of China (No. 21967004 and 22361046) and the Open Fund of Guangxi Key Laboratory of Agricultural Resources Chemistry and Biotechnology (2022KF03).

Notes and references

1 M. Liu, L. Zhang and T. Wang, Supramolecular chirality in self-assembled systems, *Chem. Rev.*, 2015, **115**, 7304–7397.
2 G. Liu, M. G. Humphrey, C. Zhang and Y. Zhao, Self-assembled stereomutation with supramolecular chirality inversion, *Chem. Soc. Rev.*, 2023, **52**, 4443–4487.
3 J. Li, Y. Cui, Y. L. Lu, Y. Zhang, K. Zhang, C. Gu, K. Wang, Y. Liang and C. S. Liu, Programmable supramolecular chirality in non-equilibrium systems affording a multistate chiroptical switch, *Nat. Commun.*, 2023, **14**, 5030.
4 T. Hirao, S. Kishino and T. Haino, Supramolecular chiral sensing by supramolecular helical polymers, *Chem. Commun.*, 2023, **59**, 2421–2424.
5 K. Wang, X. Tian, J. H. Jordan, K. Velmurugan, L. Wang and X. Y. Hu, The emerging applications of pillararene architectures in supramolecular catalysis, *Chin. Chem. Lett.*, 2022, **33**, 89–96.
6 X. Dou, N. Mehwish, C. Zhao, J. Liu, C. Xing and C. Feng, Supramolecular hydrogels with tunable chirality for promising biomedical applications, *Acc. Chem. Res.*, 2020, **53**, 852–862.
7 L. Zhang, H. X. Wang, S. Li and M. Liu, Supramolecular chiroptical switches, *Chem. Soc. Rev.*, 2020, **49**, 9095–9120.
8 G. Liu, S. Guo, L. Liu, Y. Fan, Z. Lian, X. Chen and H. Jiang, Shape-persistent triptycene-derived pillar[6]arenes: synthesis, host–guest complexation, and enantioselective recognitions of chiral ammonium salts, *J. Org. Chem.*, 2023, **88**, 10171–10179.
9 A. Chen, Y. Zhong, X. Yin, R. Li, Q. Deng and R. Yang, A novel achiral fluorescent nanoprobe for the chiral recognition of cysteine enantiomers, *Sens. Actuators, B*, 2023, **393**, 134262.
10 Y. Q. Jiang, K. Wu, Q. Zhang, K. Q. Li, Y. Y. Li, P. Y. Xin, W. W. Zhang and H. M. Guo, A dual-responsive hyperbranched supramolecular polymer constructed by cooperative host–guest recognition and hydrogen-bond Interactions, *Chem. Commun.*, 2018, **54**, 13821–13824.
11 J. Li, X. Han, X. Kang, Y. Chen, S. Xu, G. L. Smith, E. Tillotson, Y. Cheng, L. J. McCormick McPherson, S. J. Teat, S. Rudic, A. J. Ramirez-Cuesta, S. J. Haigh, M. Schroder and S. Yang, Purification of propylene and ethylene by a robust metal-organic framework mediated by host–guest interactions, *Angew. Chem., Int. Ed.*, 2021, **60**, 15541–15547.
12 G. Travagliante, M. Gaeta, R. Purrello and A. D'Urso, Recognition and sensing of chiral organic molecules by chiral porphyrinoids: a review, *Chemosensors*, 2021, **9**, 204.
13 O. N. Kataeva, K. E. Metlushka, Z. R. Yamaleeva, K. A. Ivshin, A. G. Kiiamov, O. A. Lodochnikova, K. A. Nikitina, D. N. Sadkova, L. N. Punegova, A. D. Voloshina, A. P. Lyubina, A. S. Sapunova, O. G. Sinyashin and V. A. Alfonsov, Co-ligand induced chiral recognition of n-thiophosphorylated thioureas in crystalline ni(ii) complexes, *Cryst. Growth Des.*, 2019, **19**, 4044–4056.
14 A. V. Gonzalez, M. C. B. Aniceto, M. P. Sierra, F. Sanchez, A. Arnanz, M. Boronat and M. Iglesias, BINOL-containing chiral porous polymers as platforms for enantiorecognition, *ACS Appl. Mater. Interfaces*, 2022, **14**, 53936–53946.
15 J. Wang, X. Xu, H. Chen, S. S. Zhang and Y. X. Peng, Oxidation of sodium deoxycholate catalyzed by gold nanoparticles and chiral recognition performances of bile salt micelles, *Molecules*, 2019, **24**, 4508–4521.
16 J. Tao, H. Wang, Y. Sun, X. Sun and Y. Hu, Self-assembled nanovesicles based on chiral bis-H(8)-BINOL for Fe(3+) recognition and secondary recognition of l-cysteine by 1 + 1 complex, *RSC Adv.*, 2024, **14**, 2422–2428.
17 K. Salikolimi, V. K. Praveen, A. A. Sudhakar, K. Yamada, N. N. Horimoto and Y. Ishida, Helical supramolecular polymers with rationally designed binding sites for chiral guest recognition, *Nat. Commun.*, 2020, **11**, 2311.
18 D. H. Li and B. D. Smith, Molecular recognition using tetralactam macrocycles with parallel aromatic sidewalls, *Beilstein J. Org. Chem.*, 2019, **15**, 1086–1095.
19 J. Yang, H. Wang, Q. Zhao, D. Wu, Y. Peng, L. Deng and Y. Kong, Chiral supramolecular hydrogel with controllable phase transition behavior for stereospecific molecular recognition, *J. Electroanal. Chem.*, 2021, **883**, 115045.
20 N. Song, T. Kakuta, T. A. Yamagishi, Y. W. Yang and T. Ogoshi, Molecular-scale porous materials based on pillar[*n*]arenes, *Chem*, 2018, **4**, 2029–2053.
21 C. Shi, H. Li, X. Shi, L. Zhao and H. Qiu, Chiral pillar[n] arenes: conformation inversion, material preparation and applications, *Chin. Chem. Lett.*, 2022, **33**, 3613–3622.
22 H. Zhu, Q. Li, Z. Gao, H. Wang, B. Shi, Y. Wu, L. S. Guan, X. Hong, F. Wang and F. Huang, Pillararene Host–guest complexation induced chirality amplification: a new way to detect cryptochiral compounds, *Angew. Chem., Int. Ed.*, 2020, **59**, 10868–10872.
23 W. Liu, W. Xu, H. H. Luan, G. Li, J. Liu, Z. Lu, F. Zhang and H. Li, L-ribose specific recognition surface constructed by pillar[5]arene-based host–guest interaction, *Biosens. Bioelectron.*, 2023, **241**, 115678.
24 L. Liu, C. Ma, Q. He, Y. Huang and W. Duan, Effective enantiomeric identification of aromatic amines by tyrosine-modified pillar[5]arenes as chiral NMR solvating agents, *Org. Chem. Front.*, 2021, **8**, 4144–4152.
25 P. Rajasekar, C. Jose, M. Sarkar and R. Boomishankar, Effective enantioselective recognition by chiral amino-phosphonium salts, *Angew. Chem., Int. Ed.*, 2021, **60**, 4023–4027.

26 A. K. Gupta, J. Nicholls, S. Debnath, I. Rosbottom, A. Steiner and R. Boomishankar, Organoamino phosphonium cations as building blocks for hierarchical supramolecular assemblies, *Cryst. Growth Des.*, 2011, **11**, 555–564.

27 L. Liu, W. Duan, Y. Kou, L. Wang, H. Meier and D. Cao, Crystal structure and host–guest binding ability of three types of pillar[5]arenes, *Chin. J. Chem.*, 2015, **33**, 346–350.